Prabha Materials Science Letters
Vol. 3, No. 2, 218-241, 2024
https://doi.org/10.33889//PMSL.2024.3.2.014

Ram Arti Publishers

A Review on the Magnetic Behaviour of Ni and Mn based Double Perovskites

Amit Kumar Singh
Department of Physics,
Marwari College, Lalit Narayan Mithila University, 846004, Darbhanga, Bihar, India.
Corresponding author: amitphy1991@gmail.com

Ashwani Kumar
Department of Physics,
Regional Institute of Education (NCERT), 751022, Bhubaneswar, Odisha, India.
E-mail: 01ashraj@gmail.com

Beer Pal Singh
Department of Physics,
Chaudhary Charan Singh University Meerut, 250005, Meerut, Uttar Pradesh, India.
E-mail: drbeerpal@gmail.com

(Received on July 7, 2024; Revised on July 15, 2024; Accepted on July 16, 2024)

Abstract
This review article describes the observation of some fascinating phenomena in double perovskites. Multifunctional double perovskite materials of general formula $A_2BB'O_6$ have received significant scientific attention owing to their fascinating physical characteristics, such as low field magnetoresistance, high temperature ferromagnetism, metal-insulator transition, spin ordering, phase separation and multiferroicity making them a potential candidate for spintronics device applications. Among them, R_2NiMnO_6 double perovskites have drawn significant attention in last few decades, owing to their rich physics and potential applications. The ordered arrangement of B-site cations is essential for unlocking unique magnetic and transport characteristics in these compounds. While double perovskites with ordered B-sites are highly sought after for their magnetoresistive and ferromagnetic (FM) properties, achieving perfect order is challenging due to the similarity in ionic radii and oxidation states among various cations at the B-site, leading to randomness in the arrangement of ions. This results in the occurrence of "anti-site" disorders, where the arrangement becomes random. These disorders may manifest as Ni^{2+}-O–Ni^{2+} and Mn^{4+}–O–Mn^{4+} configurations, causing antiferromagnetic (AFM) interactions in R_2NiMnO_6. Furthermore, the development of antiphase boundaries (APBs) owing to anti-site disorders may be the primary source of antiferromagnetic interaction in R_2NiMnO_6. These antisite disorders strongly affect the properties of the double perovskites and lead to the origination of some fascinating phenomena such as exchange bias and spin glass. These phenomena are utilized in the development of spintronic devices. The discussion made in the present review article would be extremely helpful to the researchers who are doing research in the field of material science.

Keywords- Double perovskite, Antisite disorder, Magnetism, Spin glass, Exchange bias.

1. Introduction

Research on multifunctional materials is essential due to their significance in various crucial fields such as multiferroicity, fuel cells, and spintronics (Chauhan et al., 2016; Kumar et al., 2017; Li et al., 2015; Mishra et al., 2014; Balasubramanian et al., 2018; Singh et al., 2020). **Figure 1** depicts the schematic diagram of various kinds of multifunctional materials. Intensive studies of ferroelectric (FE) and ferromagnetic (FM) materials have led to significant scientific and technological advances (Azuma et al., 2005; Sharma et al., 2013b; Vijayasundaram et al., 2016; Vashisth et al., 2017; Zhang et al., 2023; Zhou et al., 2020). Ferroelectricity can originate from mechanisms like charge ordering, octahedral distortion, strain mediation, and geometrical frustration (Kimura et al., 2003a). It typically involves the movement of positive and negative ions creating surface charges, often requiring empty d orbitals. Nevertheless, magnetism is related to the electron spins in partially filled d orbitals. Ferroelectric materials are utilized in capacitors

with high dielectric constants, transducers, actuators, and memory devices, leveraging their hysteresis properties for stable polarization states (Guo et al., 2014; Kimura et al., 2003a; Lu and Qi, 2019; Vijayasundaram et al., 2016). Ferromagnetic materials are essential in a lot of engineering applications, like sensors, read heads, and memory devices (Asai et al., 2005; Gajek et al., 2005; Jonker and Van Santen, 1950; Zhou et al., 2011). Furthermore, Magnetoelectric (ME) multiferroics (MF) are also multifunctional materials that show both ferromagnetic and ferroelectric characteristics, enabling linear coupling (Čebela et al., 2017; Kimura et al., 2003b; Nair et al., 2020; Sharif et al., 2021). This unique combination has gained substantial interest owing to its fundamental physics and possible applications such as magnetic sensors, memory devices, energy storage devices, actuators, and photovoltaics. ME materials can achieve strong ME coefficients through the interplay of different ferroic order parameters, offering other functional parameters and enabling multiple logic states for various applications. These materials integrate the characteristics of their FE and FM components while exhibiting unique properties. The ability to control charges with magnetic fields and spins with electric fields opens up possibilities for innovative multifunctional devices (Čebela et al., 2017). Heusler compounds are another class of multifunctional materials, known for their diversity, with over 1000 known members. These ternary intermetallic exhibit strong d nature of bands near the Fermi energy and various local and hybridized moments in the 4f -shell, leading to vital properties such as magnetic, topological, superconducting, magnetoelastic, heavy fermion, and thermoelectric characteristics (Husain et al., 2017; Kawasaki et al., 2022; Kim et al., 2013; Mishra et al., 2014; Moya et al., 2006; Sharma et al., 2013a;Yadav and Chaudhary, 2015). These properties are often explained through simple electron counting rules (Graf et al., 2011). The dependency of properties on compositions, along with strong coupling to lattice distortions, makes Heusler compounds a promising applicant for material designing (Kawasaki et al., 2022).

The increasing demand of energy and environmental concerns have driven the search for sustainable solutions in unpolluted energy applications. Developing multifunctional materials with both electric and magnetic orderings aims to reduce power consumption and enhance functionality for future electronic devices (Gajek et al., 2005). Perovskite materials are particularly promising due to their diverse physical properties, making them suitable for theoretical modeling and practical applications such as spintronics, electrodes, solar cells, sensors, memory devices, lasers, and fuel cells (García-Landa et al., 1999; Kobayashi et al., 1998; Tomioka et al., 2000). Oxides with an ABO_3 type perovskite structure have drawn significant consideration for their magnetoresistance, ferroelectricity, and superconductivity (Čebela et al., 2017; Torrance et al., 1992; Zhong et al., 2013). In the last few decades, perovskites have also been utilized as electrodes for fuel cells, especially those have two types of cations at the B site. Recently, a focus has been on discovering new magnetic materials for applications in spintronics, magneto-caloric materials, hard magnets, and multiferroics. Double perovskites having formula $A_2BB'O_6$, featuring an ordered arrangement of BO_6 and $B'O_6$ units, are versatile compounds for this purpose (Kato et al., 2002; Saha-Dasgupta, 2013; Vasala and Karppinen, 2015). By selecting appropriate metal ions B and B', along with rare earth ions A, a vast variety of physical characteristics can be achieved (Vasala and Karppinen, 2015). Noteworthy compound include Sr_2FeMoO_6 and Sr_2FeReO_6, which are half-metals with high Curie temperatures (T_C) and notable magneto resistive properties (Serrate et al., 2006). These properties result from the combination of localized 3d ions at the B site and delocalized 4d or 5d ions at the B' site. Another important candidate of the double perovskite family, Sr_2CrOsO_6, is a ferrimagnetic insulator with an exceptionally high T_C ~720 K, illustrating the requirement for discovering new magnetic materials among double perovskites.

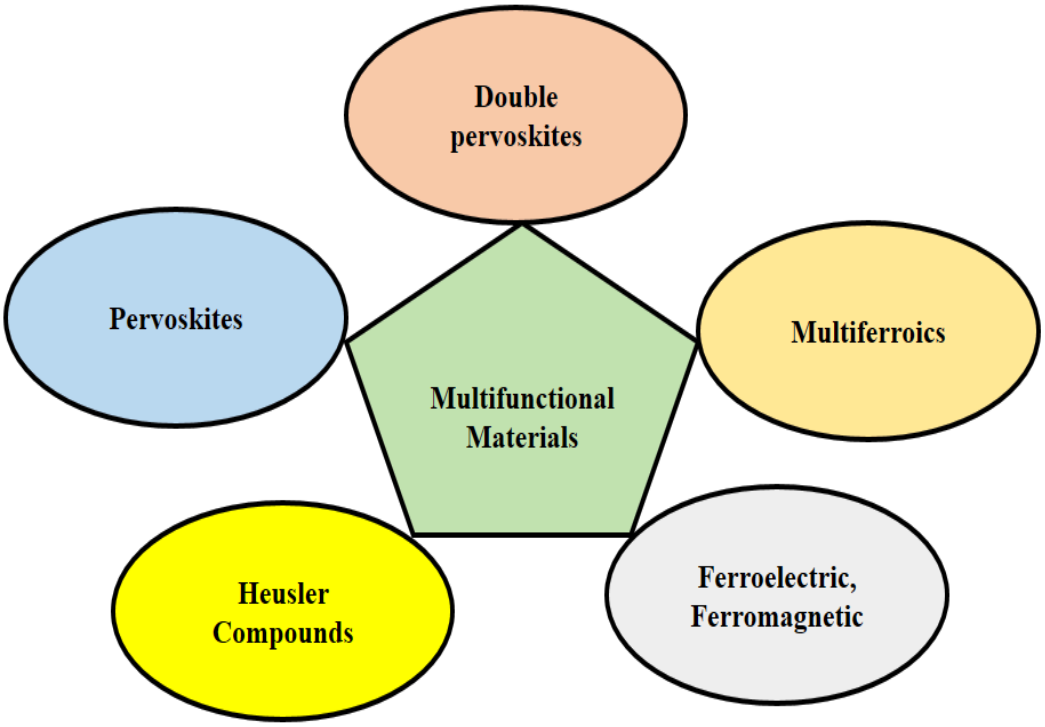

Figure 1. Schematic diagram of various kinds of multifunctional materials.

1.1 Perovskites

In the last few decades, Perovskite oxides are intensely studied owing to vast variety of electrical, optical, and magnetic characteristics (Imada et al., 1998; Salamon and Jaime, 2009). Jonker and Van Santen (1950), while studying manganites ($AMnO_3$) first reported the oxide perovskites with near room temperature ferromagnetism. The occurrence of mixed valence states of Mn in these compounds, allows transfer of electrons between oxygen orbitals, which was invoked to further describe the ferromagnetism through a double exchange interaction (Zener, 1951). Additionally, on applying a magnetic field significant reduction in resistance has been observed in these materials (von Helmolt et al., 1993). This negative magnetoresistance has opened the window for the current research on colossal magnetoresistive materials, which are applicable in magnetic storage devices (von Helmolt et al., 1993). Further, Muller and Bednorz, discovered the superconductivity in copper oxides and accelerated the research in the area of doped perovskites (Bednorz and Muller, 1986).

The ideal perovskite structure, ABO_3, where, *A*, and *B* are cations and *O* is anion, respectively. In ABO_3, B ions occupy the center of oxygen octahedra, arranged in a corner-sharing configuration. A type ion is located in the remaining space at the center and typically have a lesser direct impact on the characteristics of the perovskite compared to the $[BO_6]$ octahedra, as depicted in **Figure 2**. Owing to their atomic arrangement perovskite oxides shows features such as multiferroicity, piezoelectricity, ferroelectricity, etc.

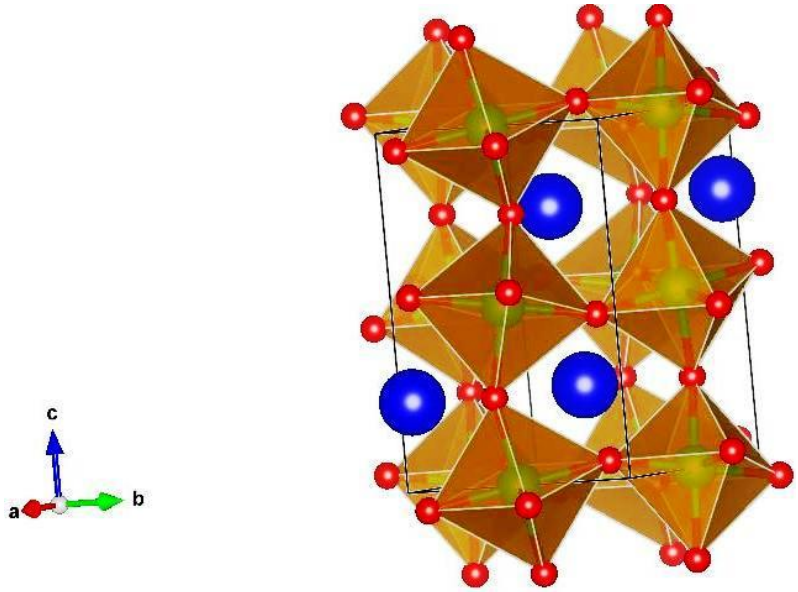

Figure 2. Simple cubic perovskite ABO_3 structure, A ions (blue spheres) are surrounded by octahedral arrangements of oxygen atoms (red spheres), with a central B ion (golden sphere).

1.2 Double Perovskites

Research on the double perovskites dates back to the early 1950s, as evidenced by studies conducted by Fresia et al. (1959), as well as Galasso et al. (1959). This structure is formed by combining alternate unit cells of two distinct perovskites. Its general formula is $A'A''B'B''O_6$, where different species are permissible for both the A and B cations, indicated by the primes. When A'=A" and B '=B", the structure simplifies to the previously described perovskite. A wider range of characteristics can be found by changing the B cations, and extensive investigations involving virtually every transition metal and 4f element have been conducted. For example, half-metallic Sr_2FeMoO_6 shows high ferromagnetic T_C (~420 K) with large low field magnetoresistance (MR) (García-Landa et al., 1999; Kobayashi et al., 1998; Tomioka et al., 2000). Thus, in such systems, it is typically the B cations that undergo differentiation, with two or more distinct species chosen, as this is where the intriguing physics and chemistry emerge.

Double perovskite structures can adopt three distinct arrangements of B cations (Vasala and Karppinen, 2015), illustrated in **Figure 3**. The first arrangement involves an alternate placement of B' and B" cations at the center of oxygen octahedra, referred to as the rock salt or 1:1 type ordered structure. The second array features a layered structure where layers consist of either only B' or only B" at the center of the octahedra. In the third scenario, a columnar ordering occurs, with alternating B cations in two directions. The second type is exceptionally rare and was initially synthesized in 1990 in La_2CuSnO_6 (Anderson and Poeppelmeier, 1991), followed by Sr-doped $La_{2-x}Sr_xCuSnO_6$ (Anderson et al., 1993a), and subsequently in Ln_2CuMO_6 (Ln = La, Nd, Pr, and Sm; M = Zr and Sn) (Azuma et al., 1998). Only six compounds were identified in fifty years of research on double perovskite materials. Accompanying the successful formation of the layered structure, Anderson et al. (1993b), collected data from over 300 studies since the 1950s to propose the probable structure for a new compound.

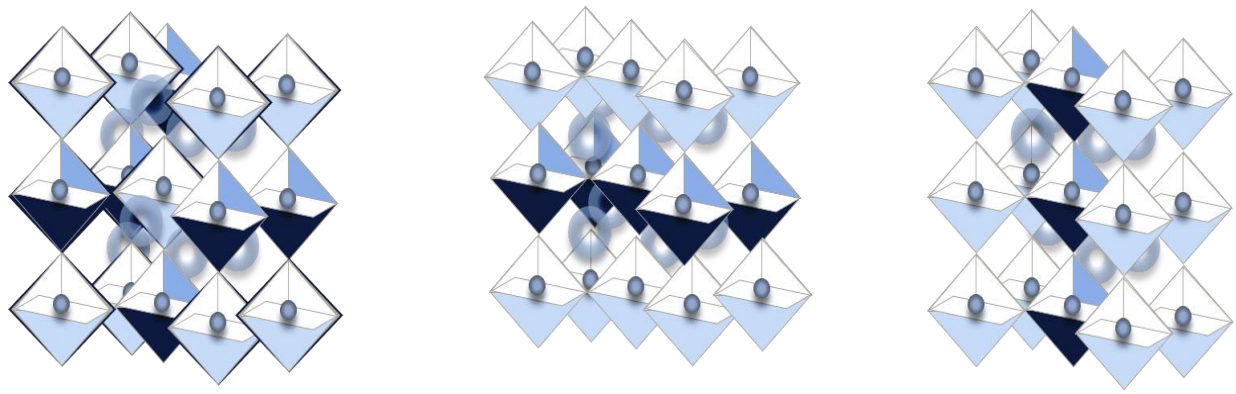

Figure 3. Different types of $A_2B'B''O_6$ double perovskites: (a) rock-salt, (b) layered and (c) columnar order.

They emphasized that the primary determinant of the B cation arrangement was the charge disparity, with ionic radii difference being the secondary factor (Vasala and Karppinen, 2015). As the variance in valence states between the two B cations increases, the preference leans towards a 1:1 type ordered or rock salt arrangement. Moreover, an increase in the disparity of ionic radii between the two B cations also favors the 1:1 ordering. It can be simplified as: as the B cations become more alike, their specific placement becomes less significant, leading to a tendency towards randomness in the arrangement of ions. Specifically, for charge differences exceeding 2, the ordered arrangement is favored, while for differences less than 2, the random array is more favorable condition. When charge differences are exactly 2, the ordered arrangement prevails if the ionic radii difference exceeds 0.2 Å; otherwise, the random arrangement takes place.

The structure and characteristics of the system can be decided by the selection of *B* cations. After selecting the B cations, the choice of the A cation is primarily determined by its dimension and its capacity to stabilize the perovskite structure. Goldschmidt, presented a parameter '*t*' to assess the probable stability of a perovskite compound, based on simple geometrical considerations (Goldschmidt, 1926). Equation (1) has been adapted for the double perovskite:

$$t = \frac{\left[\frac{r_{A'}+r_{A''}}{2}\right] + \langle r_O \rangle}{\sqrt{2}\,[(\frac{r_{B'}+r_{B''}}{2}) + r_O]} \quad (1)$$

where, $r_{A'}$, $r_{A''}$, $r_{B'}$, $r_{B''}$, and r_O are the ionic radii of the ions. As the parameter 't' approaches unity, the structure becomes cubic; however, as '*t*' decreases from 1, the structure becomes increasingly distorted. This distortion leads to tension in the A-O bonds and compression in the B-O bonds, resulting in the octahedral tilting to partially relieve these strains. Large A cations are chosen to reduce strain and accommodate the $[BO_6]$ octahedra comfortably within the double perovskite structure. While the model is simplistic and doesn't consider the properties of individual ions, typically a '*t*' value below 0.9 suggests that a structure other than perovskite may be more favorable (Schmitz-DuMont and Kasper, 1965). Besides size, A cations are selected for their ability to affect the valence state of B cations, which significantly impacts material properties. Hence, numerous studies have replaced La^{3+} with Sr^{2+} due to their similar size but different valence states, leading to compensating variations in the valences of B cations (Anderson et al., 1993a; Schmitz-DuMont and Kasper, 1965; Kang et al., 2009; Murthy and Venimadhav, 2013). In a perfect double perovskite with cubic structure (t = 1), A type cations are twelve-coordinated, with four oxygen anions in each layer (Glazer, 1972). However, tilting and octahedral distortion typically reduce the coordination number of A cations to 8-10. Glazer classified the tilting, distortion of octahedra, and dislocations of A or B cations (Glazer, 1972). In $A_2BB'O_6$ structure, there are partially filled orbitals of B and empty orbitals of

B' or vice-versa. There occurs 180°-superexchange through the oxygen ions between B and B' cations resulting in ferromagnetic insulator behaviour (Dass et al., 2003). Many unique functional properties are originated by the ordered array of B and B' ions in $A_2BB'O_6$ structure. To attain the ordered array of B and B' ions in double perovskite compound is very difficult. Normally, perovskite compound exhibits antiferromagnetic insulating behaviour but when it is doped with manganese, it shows ferromagnetic semiconducting behaviour by developing a double perovskite compound (Vasala and Karppinen, 2015). Hence, most of the perovskites are antiferromagnetic insulator, while double perovskite compounds exhibit ferromagnetic semiconducting nature (Booth et al., 2009; Salamon and Jaime, 2009).

Materials, which possess co-existing magnetic and electric orderings are of main importance for potential applications in electronic devices. Ni and Mn based double perovskites i.e. R_2NiMnO_6 (RNMO, R=rare earth element) type ferromagnetic (FM) double perovskites are such multifunctional materials, which have drawn significant consideration owing to the rich physics leading to diverse properties such as ferromagnetism, spin glass, ferroelectricity, near room temperature magnetoresistance and magnetoelectricity and multiferroicity (Choudhury et al., 2012; Singh et al., 2011; Wang et al., 2009; Yang et al., 2012). These materials also show a large spin-lattice coupling leading to multiferroicity. The complex and rich physical characteristics can be utilized in fabricating multiferroics and investigating the basic coupling behaviour for device applications from a fundamental perspective.

2. R_2NiMnO_6 Double Perovskites

R_2NiMnO_6 is a distinct group of double perovskites (Anderson et al., 1993a) where, ferromagnetic ordering of d-electron spins arises due to a near-ideal e_g^2-O-e_g^0 electronic interaction, as per the classical rule of Goodenough–Kanamori (Goodenough, 1955; Kanamori, 1959). Out of them, La_2NiMnO_6 compound, having a high Curie temperature (T_C) of 280 K, has been in focus in recent years (Chandrasekhar et al., 2012; Dass et al., 2003; Joly et al., 2002; Rogado et al., 2005), owing to the observation of multiple properties and also due to the possibility that the basic understanding of its interaction may give new directions towards designing of multifunctional compounds like Bi_2NiMnO_6 (Azuma et al., 2005) and (La, Lu)$NiMnO_6$ (Singh and Park, 2008). La_2NiMnO_6 (LNMO) compound is rigorously explored in bulk and thin film forms (Choudhury et al., 2012; Guo et al., 2006, 2008; Guo et al., 2013a; Singh et al., 2007), however, other R_2NiMnO_6 oxides are less explored (Booth et al., 2009; Singh et al., 2011; Yang et al., 2012; Yadav and Elizabeth, 2015). Although, oxides of this series are FM with T_C lower than that of the LNMO but the connections between structure and physical property mainly for the relation between R^{3+} and $NiMnO_6$ system for the oxides of this family has not been completely studied. While R = La, Y and Nd members of this series exhibit ordered monoclinic (space group) P21/n structure (Mouallem-Bahout et al., 2004; Rogado et al., 2005), the orthorhombic (Pnma) structure is reported for other members (Bull and McMillan, 2004) indicating an partial Ni and Mn ordering. Ni and Mn ordering was supposed (but not found) by Asai et al. (1998) in their study on the magnetic behaviour of all the members of this family. Furthermore, it has also been noted that substituting La with a smaller rare earth element result in alterations to the (Mn-O-Ni) bond length and bond angles, thereby modifying exchange interactions (Booth et al., 2009). Thus, it is possible to control the physical characteristics of these materials by varying the Ni-O-Mn bonds length and bond angles. Super-exchange interaction between ordered Ni^{2+} and Mn^{4+} cations leads to FM behaviour in these compounds while the anti-site disorders yield Ni^{2+}-O^{2-}-Ni^{2+} and Mn^{4+}-O^{2-}-Mn^{4+} interactions and, thereby, generating antiferromagnetic ordering (Yadav and Elizabeth, 2015). Thus, the presence of both FM and AFM phases together could lead to some interesting phenomena such as exchange bias in these compounds. To study the magnetic behaviour of double perovskites, it is necessary to know the crystal structure of the double perovskite compounds. In this regard, we have considered an example of Nd_2NiMnO_6 (NNMO) to explain the magnetism in R_2NiMnO_6 family of double perovskites. The crystal structure of NNMO is showed in **Figure 4**.

Double perovskite NNMO grows in P21/n space group (Yadav and Elizabeth, 2015). The unit cell is two times that of a single perovskite cell with lattice constants $a \sim b \sim \sqrt{2}a_p$ and $c = 2a_p$; where a_p is the lattice parameter of the cubic perovskite cell ABO_3 (Singh et al., 2010). In completely ordered double perovskite structure, the Ni and Mn ions alternate periodically in three dimensions. Both the transition metal ions are bounded by six oxygen atoms, creating an octahedral network in a rock salt like manner (Singh et al., 2010). The MnO_6 and NiO_6 octahedra layers are corner shared by in-plane oxygen ions (O2, O3) and the apical oxygen ions (O1). The Nd atom occupies the centre between the eight octahedron **Figure 4**) and is thus coordinated by 12 oxygen atoms. The Mn and Ni atoms occupy distinct crystallographic positions *2b* and *2c*. In a unit cell, the coordinates of Mn atoms are (1/2 0 0) (0 1/2 1/2) and Ni atoms occupy (0 1/2 0) and (1/2 0 1/2) positions (Nair et al. 2014). However, the Ni-O bond-lengths are slightly larger by nearly 0.1 Å (Saha-Dasgupta, 2013). Shi et al. (2011), found that NNMO exhibits FM behaviour with a T_C of approximately 194 K, caused by Ni^{2+}-O-Mn^{4+} superexchange interactions. An additional magnetic transition near 105 K has been detected, caused by Ni^{3+}-O-Mn^{3+} super exchange interactions. The magnetic properties of NNMO can potentially lead to the formation of Ni/Mn cation ordering in NNMO. For NNMO, two main concerns arise: (i) Ni and Mn valence states and (ii) exchange interaction giving ferromagnetic ordering. Regarding the valences, there are two prospects: Ni^{3+}–Mn^{3+} and Ni^{2+}–Mn^{4+}. In octahedral symmetry, Ni^{2+}–Mn^{4+} combination exhibit electronic configurations of $d^8(t_{2g}^6 e_g^2)$-$d^3(t_{2g}^3)$, while Ni^{3+}–Mn^{3+} combination display electron configurations $d^7(t_{2g}^6 e_g^1)$-$d^4(t_{2g}^4)$ or $d^7(t_{2g}^6 e_g^1)$-$d^4(t_{2g}^3 e_g^1)$. The exchange interaction is determined by the sign of the superexchange interaction, governed by Ni and Mn valence states in accordance with the Goodenough–Kanamori–Anderson (GKA) rules (Goodenough, 1955; Kanamori, 1959). These rules predict that ferromagnetism arises from the interaction between the unoccupied d orbital of one metal site and the half-filled d orbital of another metal site via an anion in a 180° super exchange interaction. Specifically, the GKA rules suggest that the Mn^{4+}- Ni^{2+} interaction is ferromagnetic, with interactions involving e_g orbitals dominating over those involving t_{2g} orbitals owing to larger cation-anion overlap. The super exchange interaction between filled e_g^2 and vacant e_g states yields ferromagnetic character, as shown in **Figure 5**.

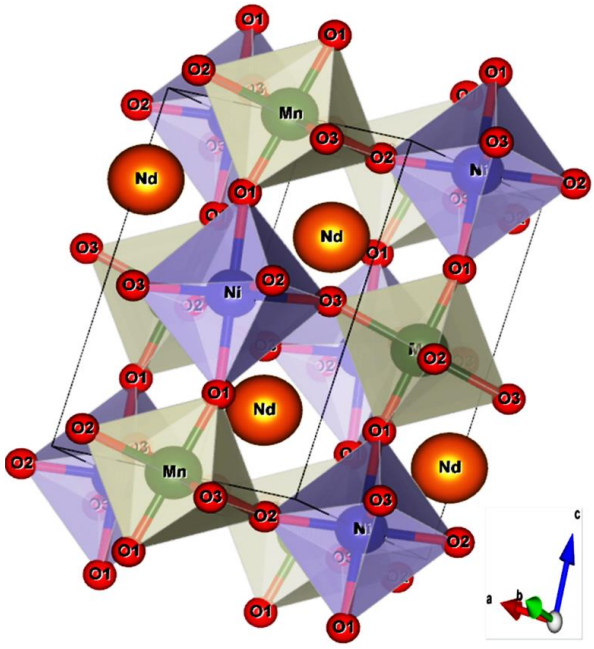

Figure 4. Crystal structure of Nd_2NiMnO_6.

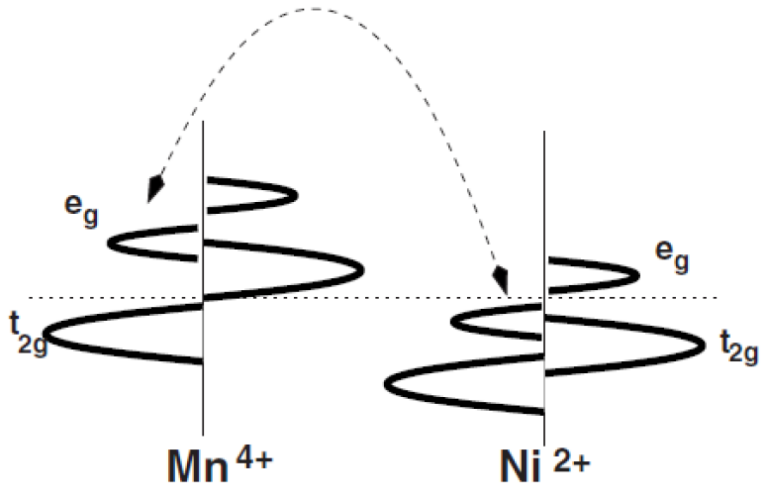

Figure 5. The GKA rules predict that the super exchange interaction between e_g orbitals leads to ferromagnetic ordering.

The magnetic order of such compounds is affected by the comparative strength of FM and AFM orderings, which are determined by the electrons in the t_{2g} and e_g orbitals. This can be understood considering superexchange interactions between Ni^{2+} and Mn^{4+}. In an octahedral coordination structure, Ni^{2+} (d^8:$t_{2g}^6 e_g^2$) has a half-filled e_g orbital, while Mn^{4+} (d^3: $t_{2g}^3\, e_g^0$) possesses a half-filled t_{2g} orbital and a vacant e_g orbital. Superexchange interactions takes place through virtual hopping between the half-filled Ni-e_g and vacant Mn-e_g orbitals, as well as between the half-filled Mn-t_{2g} orbitals, leading to FM and AFM orderings, respectively. When the <Ni-O-Mn> bond angle is 180°, virtual hopping between Ni-e_g and Mn-e_g orbitals promotes FM character, whereas for a 90° bond angle, hopping between Ni-e_g and Mn-t_{2g} orbitals yields antiparallel alignment of spin. Electron hopping between Ni-e_g and Mn-t_{2g} orbitals strengthens with diminishing the bond angle. On the other hand, hopping between Ni-e_g and Mn-e_g orbitals deteriorates with decreasing the bond angle. Consequently, the T_C decreases as the <Ni-O-Mn> bond angle reduces.

3. Antisite Disorders

In double perovskites, both B and B' ions are coordinated by six oxygen atoms and situate at the center of oxygen octahedral (Vasala and Karppinen, 2015). There should be another array of B and B' ions manner along each cubic axis in structurally ordered double perovskite. Although there is dissimilarity between B and B' ions, there always occurs large chances of mislocation (Nair et al., 2014; Singh et al., 2016; Vasala and Karppinen, 2015). The B' site may be filled by B ion and conversely. This possibility is not present in the perovskites due to only one type of 'B ion'. The unavoidable 'antisite disorders' (ASDs) have to be assumed in the synthesis of the double perovskites. The origin of magnetic ordering in structurally ordered materials is due to a combined effect of delocalization of electron on B-O-B' network and strong electron-spin coupling on the B ion (Vasala and Karppinen, 2015). The magnetic ordering is influenced by the arrangement of B and B' ions. Two adjacent B ions, resulting from mis location, normally possess an AFM superexchange interaction between the ions (Dass et al., 2003; Singh et al., 2016; Wang et al., 2009). Such interaction can significantly improve the physical properties, including magnetic order and transport properties (Dass et al., 2003; Singh et al., 2016; Wang et al., 2009).

Antisite disorders are natural growth defects in double perovskite compounds (Singh et al., 2017c; Singh and Chandra, 2018; Singh et al., 2017a, 2017b; Singh et al., 2018). Ferromagnetism in double perovskites is elucidated by the Goodenough-Kanamori rules, which govern the exchange paths involving B^{2+}-O-B'^{4+} interactions (refer to **Figure 6 (a)**). However, achieving perfect ordering of the B^{2+}-O-B'^{4+} cations in the 2c (0 1/2 0) and 2d (1/2 0 0) Wyckoff positions, as assumed, is rarely realized in actual samples. Laboratory-prepared samples typically exhibit ASDs, where transition metal ions interchangeably hold the 2c and 2d positions (see **Figure 6 (b)**). These disorders lead B-O-B and B'-O-B' exchange interactions, thus impacting the ideal ferromagnetism of the otherwise ordered lattice by inducing antiferromagnetic clusters (Dass et al., 2003; Wang et al., 2009), consequently reducing T_C and saturation magnetization (Guo et al., 2013c). The result of disorders on the magnetic behaviour of double perovskites has been extensively investigated, particularly in compounds like La_2CoMnO_6 and LNMO (Guo et al., 2013b; Kang et al., 2009; Murthy et al., 2016; Sahoo et al., 2016). For instance, the domain structure of La_2CoMnO_6 featuring two discernible ferromagnetic regions was found (Truong et al., 2007). The almost ordered ferromagnetic phase exhibited a T_C of approximately 226 K, while the secondary magnetic phase had a T_C below 150 K. Similarly, atomic disorder and the development of antiphase boundaries (APBs) were noted in LNMO (Dass et al., 2003). The amount of anti-site disorder is influenced by factors such as cationic mismatch, the character of B and B' ions, and growth parameters (Singh et al., 2016; Wang et al., 2009). Parameters like synthesis and annealing temperature, as well as the annealing time, show pivotal roles in deciding the degree of ordering (Dass et al., 2003; Singh et al., 2016; Wang et al., 2009). Antisite disorders may arise owing to inadequate duration of annealing at lower temperatures, excessive annealing at significantly higher temperatures, or local variations in the amount of B and B' ions resulting in the development of B/B'-rich regions (Sanyal et al., 2008; Singh et al., 2016).

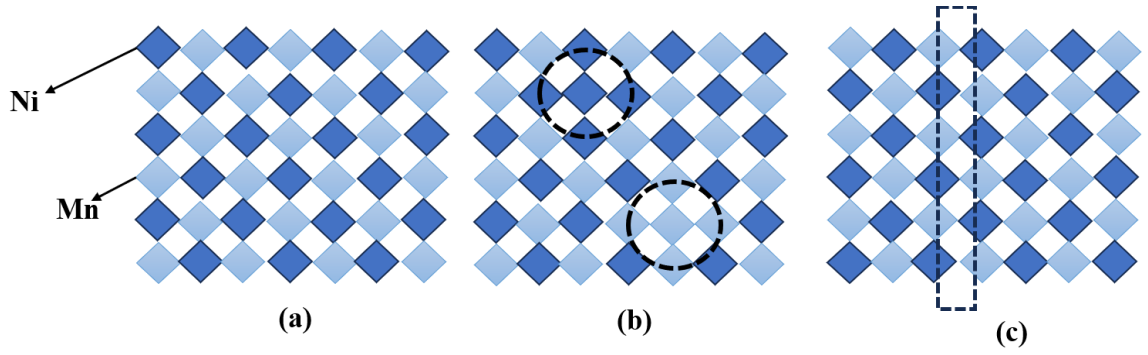

Figure 6. Different schemes of B-site cation disorder: (a) completely ordered, (b) antisite disorder and (c) antiphase boundary.

To enhance the degree of ordering, it is necessary to carefully consider the parameters of temperature and duration during annealing. Research suggests that the amount of ordering primarily rises with increasing annealing temperature but then declines (Sanyal et al., 2008). Each double perovskite system has a critical temperature at which maximum ordering occurs. By optimizing synthesis and annealing conditions, it is possible to mitigate the formation of antisite disorders. These disorders can result in the creation of antiphase boundaries illustrated in **Figure 6(c)**, which are believed to be a primary cause of antiferromagnetic coupling in these materials (Dass et al., 2003; Singh et al., 2016; Wang et al., 2009).

The presence and extent of ASDs and antiferromagnetic APBs are notably influenced by the grain size (Wang et al., 2009). When the grain size is too small, ASDs are sparsely dispersed within each grain, resulting in feeble magnetic interaction among them. However, as temperature increases, grains have a

tendency to develop promptly, leading to the development of a larger number of antisite disorders with stronger antiferromagnetic interaction within each grain. This phenomenon gives rise to the growth of both antiferromagnetic and ferromagnetic moments (Wang et al., 2009).

4. Magnetic Phases in Double Perovskites

A range of magnetic phases arises from the numerous possible combinations of B and B' cations in double perovskites. Some examples include:
-Ferromagnets (see **Table 1**).
-Antiferromagnets (see **Table 2**).

Spin glass phase observed in compounds like Sr_2FeCoO_6 (Pradheesh et al., 2012) and Ba_2YMoO_6 (De Vries et al., 2010).

Additionally, double perovskites can exhibit superconductivity. For instance, the partially melted ceramic material $Sr_2YRu_{0.85}Cu_{0.15}O_6$ displays superconductivity with an onset temperature of T_C around 45 K (Blackstead et al., 2001; Galstyan et al., 2007) under ambient pressure. To begin our discussion, let's provide a brief overview of ferromagnets.

4.1 Ferromagnetic Insulating Phase

In double perovskites like $A_2BB'O_6$, each B and B' occupies an octahedral scenario (BO_6 and $B'O_6$), causing a crystal field splitting of d-states into t_{2g} and e_g manifolds (Sarma et al., 1996). In Ca_2FeReO_6, the small ionic radius of Ca results in a monoclinic distortion, increasing the degeneracy of t_{2g} levels on the Re sites (each has two t_{2g} electrons). This distortion leads to a variation of the bond angle (Fe-O-Re) from 180° to approximately 156°, reducing the Re-Re overlap by misaligning the t_{2g} orbitals. Consequently, this distortion diminishes the hopping energy of d-electrons due to decreased hybridization between transition metal d and oxygen p states, resulting in the insulating behaviour of Ca_2FeReO_6 (Kato et al., 2002). LNMO is a significant member of this family, holding promise for various technological applications. It exhibits a T_C~ 280 K, near room temperature (Dass et al., 2003). Ferromagnetism arises from superexchange interactions among Mn-O-Ni (Haskel et al., 2011). The compound also displays magnetoresistance and magnetocapacitance effects (Rogado et al., 2005), indicating a coupling between different properties modifiable by applying a magnetic field. The observation of such phenomena near room temperature shapes it a compelling aspirant for practical applications.

Table 1. Double perovskites exhibiting ferromagnetism.

Material	Crystal structure	Transport property	Magnetic order T_C
Sr_2FeMoO_6	Tetragonal	Half-metallic	420 K (Tomioka et al., 2000)
Ba_2FeMoO_6	Cubic	Half-metallic	345 K (Kim et al., 2002)
Ca_2CrReO_6	Monoclinic	Insulating	360 K (Kato et al., 2002)
La_2NiMnO_6	Monoclinic	Insulating	280 K (Dass et al., 2003)

4.2 Antiferromagnetic Insulating Phase

Double perovskites exhibit antiferromagnetic and insulating nature for selected combination of B and B'. Sr_2FeWO6 is one typical member of this family (Bardelli et al., 2009). It has antiferromagnetic transition temperature T_N ~40 K. At the Fe-site the localized electrons exhibit huge exchange splitting. Antiferromagnetic insulating behaviour originates due to the coupling of Fe^{2+} sites through superexchange interaction in the absence of any delocalized electrons (Bardelli et al., 2009). The magnetic structure with a wave vector (0 1 1) may be ascribed as a set containing alternate ferromagnetic planes that are attached antiferromagnetically (Azad et al., 2002) with each other.

Table 2. Antiferromagnetic double perovskites.

Material	Crystal structure	Magnetic order T_N
Sr_2FeWO_6	Monoclinic	40 K (Bardelli et al., 2009)
Sr_2MnMoO_6	Tetragonal	13 K (Itoh et al., 1996)
Sr_2NiMoO_6	Tetragonal	1.5 K (Brixner, 1960)

4.3 Spin Glass Phase

A spin glass state is the resultant of randomness and frustration in a magnetic system. In a triangular lattice, frustration could arise as illustrated in **Figure 7**. The frustration arises in a triangular lattice because the third spin could not fulfill the condition for antiferromagnetic interaction with both the nearest neighbor spins on the other two sites. If we start populating a non-magnetic lattice with a dilute, randomly distributed magnetic atoms, the resultant system may exhibit a disordered state with no phase transition found to occur from disordered state occurring at high temperature to an ordered state found to occur at low temperature. However, at a particular temperature, the system shows phase transition that resembles a state, that might not be ordered, but distinct from the disordered state found to occur at high temperature. This type of magnetic state is called a spin-glass state which is dominated by freezing of spins in a random manner at a temperature T_g (*glassy* temperature) below which a metastable frozen state exists without normal long-range magnetic ordering (Bedanta and Kleemann, 2008).

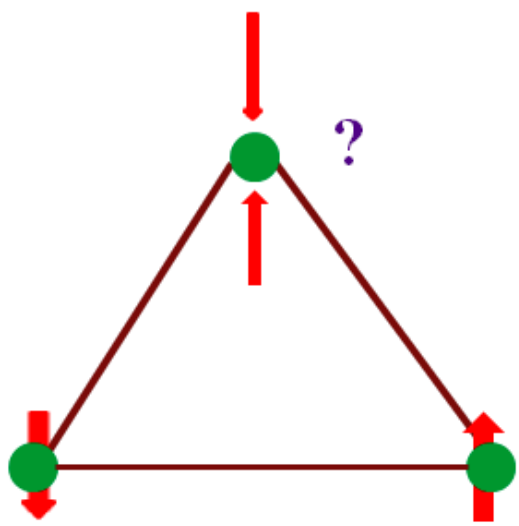

Figure 7. Frustrated antiferromagnetic configuration for a triangular lattice.

At high temperatures, the thermal fluctuations are dominant over the magnetic character of the system and all the spins behave independently (Binder and Young, 1986). However, on cooling down the system to low temperature, the fluctuations in the spins begin to decline and these spins form correlated units called domains. Further cooling of the system below T_g, the fluctuations in the domains also decline and domains begin to grow in size and the long-range glassy interactions occur between the spins while proceeding towards T_g in a boundless time limit. Thus, after approaching this phase, each spin becomes responsive of its neighboring spin and as a result, the system starts to freeze into a random frozen ground state at T_g. The spin-glass state is chaotic in behaviour (Bray and Moore, 1987) and any modification in the temperature below T_g results in a dissimilar spin configuration that could be achieved only asymptotically gradually. This forms the basis of the memory effect after ageing which is sometimes also regarded as the 'signature' of a true spin-glass behaviour.

The spin glass phase can arise from either extensive B-site disorder, such as in Sr_2FeCoO_6, or geometric frustration, as seen in Ba_2YMoO_6. In Sr_2FeCoO_6, neutron diffraction and subsequent bond valence sum study revealed random arrangement of Co and Fe at the B site, with mixed valence states of Co^{3+}/Co^{4+} and Fe^{3+}/Fe^{4+} , respectively (Pradheesh et al., 2012). The closely matched ionic radii of the B-site cations, result in significant disorder. This disorder induces a competing interaction between two adjacent neighbors in superexchange process, leading to spin frustration in the lattice and consequent spin glass behaviour.

In contrast, Ba_2YMoO_6 possesses a face-centered cubic (FCC) lattice structure. In this system, Mo exists in a 5+ oxidation state (Mo^{5+}, S = 1/2) with an individually filled degenerate t_{2g} orbital, while the Y^{3+} ion lacks a magnetic moment. The S = 1/2 Mo^{5+} moments are arranged on an FCC lattice and exhibit antiferromagnetic coupling, leading to geometric frustration. This frustration, along with quantum fluctuations, results in spin glass behaviour in Ba_2YMoO_6 (Aharen et al., 2010). Various experiments including heat capacity, ac and dc magnetic susceptibility, and muon spin rotation measurements indicate the absence of magnetic ordering below 2 K (De Vries et al., 2010).

4.4 Exchange Bias

Exchange bias (EB) phenomenon was first observed by Meiklejohn and Bean in incompletely oxidized Co particles after field cooling (Meiklejohn and Bean,1956). The EB phenomenon manifest itself as an asymmetry in the hysteresis loop in form of a shift (H_{EB}) along the axis of magnetic field. Such condition takes place, when a system consisting of AFM-FM interface is cooled down in presence of magnetic field through a temperature T such that $T_N < T < T_C$, where T_C is the Curie temperature of FM ordering and T_N is the Néel temperature of AFM ordering (**Figure 8 (a)**). The shift is accompanied by the other related observation like an increase in the coercivity (H_C), shift along the magnetization axis (M_E) (**Figure 8 (b)**), below T_N after field cooling (Berkowitz and Takano, 1999; Chaturvedi et al., 2014; Hrkac et al., 2014; Kiwi, 2001; McCord and Mangin, 2013; Meiklejohn and Bean, 1956; Nogués and Schuller, 1999; Sung et al., 2012). Unidirectional anisotropy is another related effect which is generally observed in nanoparticles and is different from uniaxial anisotropy. In unidirectional anisotropy, the angular dependence of magnetic torque (τ) is given by $K_{ud}\cos\theta$ rather than $K_{ua}\sin 2\theta$ as observed for the common uniaxial anisotropy, where, K_{ud} and K_{ua} are unidirectional and uniaxial anisotropy constants and θ is the angle between magnetization and the anisotropy axis. The presence of unidirectional anisotropy induces only one stable state (zero τ, minimum energy) instead of two stable states as observed for uniaxial anisotropy (**Figure 8 (c)**). The physical origin of this phenomenon lies in the exchange interaction among the FM and AFM parts at their interface. There are so many models to express the microscopic origin of the exchange bias due to this exchange coupling. However, in a simple manner, exchange bias could be described in the terms of the AFM spins parallel to the FM spins which takes place at their interface while field cooling process.

This could lead to two dissimilar limiting cases on the basis of the strength of the magnetic anisotropy of AFM component. For large anisotropy of the AFM component, a shift in the hysteresis loop is seen, while, in case of lower AFM anisotropy only enhancement in the coercivity is observed (without any loop shift). However, both the effects can be observed in case of structural distortions or grain size distribution which leads to local changes in magnetic anisotropy of AFM. The spin configurations for the AFM-FM components before and after field cooling is depicted in **Figure 9**. When an external magnetic field H is applied at a temperature T such that $T_C > T > T_N$, then the FM spins will follow the direction of the applied magnetic field, while, the AFM spins will be randomly oriented as the temperature is above T_N. However, the magnetic order will be set up in the AFM when the temperature goes below T_N. In the process of field cooling, interfacial FM and AFM spins are likely to interact with each other. If we assume a FM interaction at the interface (AFM-FM), then the AFM spins would like to follow the direction of the FM spins (or to

say parallel to the FM spins), while, the rest of the layer of AFM spins will arrange in an antiferromagnetic manner (antiparallel to the neighboring layer spins) to give zero net magnetization in the AFM layer.

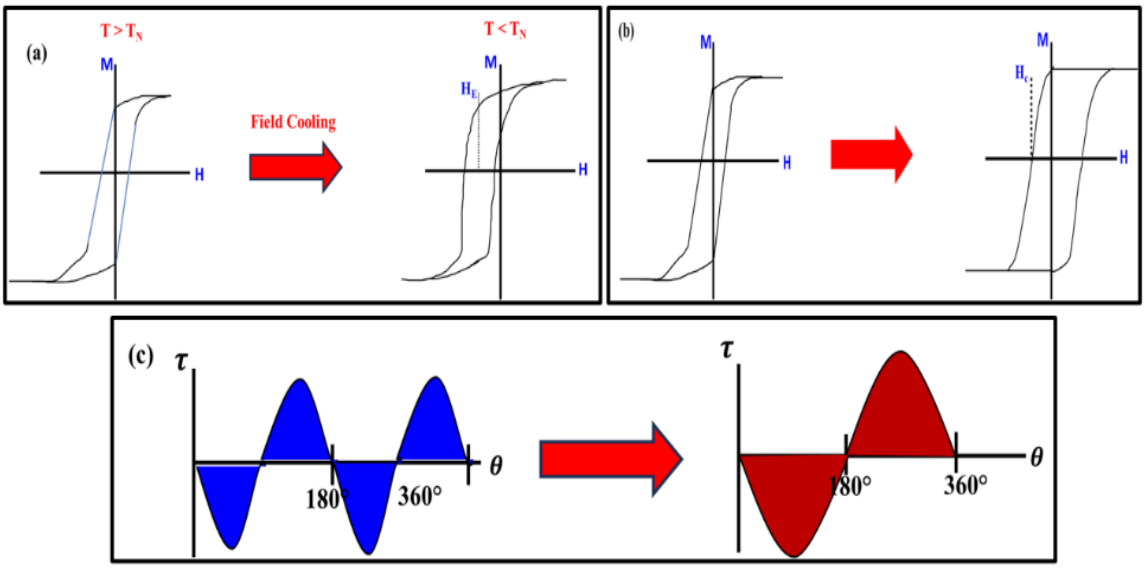

Figure 8. Main effects observed due to AFM-FM exchange coupling, (a) Hysteresis loop shift, (b) Increased coercivity, (c) Unidirectional anisotropy.

Figure 10 shows the spin configuration at various platforms when a hysteresis loop is measured for an AFM-FM system. As discussed above, the spins occurring at AFM-FM boundary lie parallel to one another after field cooling process (**Figure 10 (a)**). When the direction of the applied magnetic field is reversed, the FM spins will try to rotate in an attempt to adjust themselves in the applied field direction. However, if the magnetic anisotropy of AFM spins (K_{AFM}) is large then the AFM spins will prevail in the same situation. Subsequently, the AFM spins will apply a microscopic torque on the FM spins to maintain them in their actual way due to the interface coupling (**Figure 10 (b)**). Therefore, a comparatively large magnetic field will be needed to entirely reverse the magnetization in the FM component, then the uncoupled FM component, to surpass the torque applied by the AFM spins. This results in an increased coercivity along the negative field axis (**Figure 10 (c)**). Now, when the magnetic field is reversed back to the positive direction, it becomes easier to arrange the FM spins along the applied field as the torque applied by the AFM spins at the interface will be parallel to the applied magnetic field and hence favor the rotation of the FM spins for the magnetization reversal (**Figure 10 (d)**).

Thus, the coercivity along the positive field axis will be lesser in this case as compared to the uncoupled FM components. The net result of this process will be a shift in the hysteresis loop towards the negative field axis (H_{eb}).

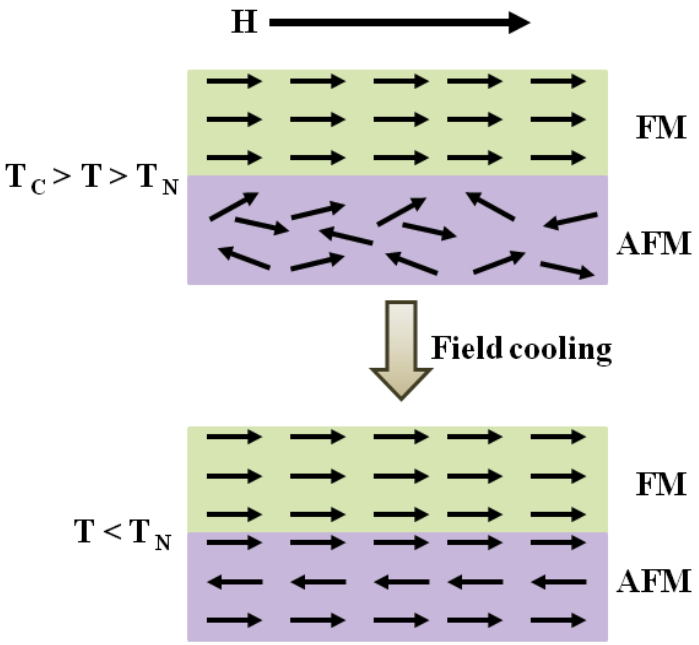

Figure 9. Spin-configuration of AFM-FM components before and after field cooling.

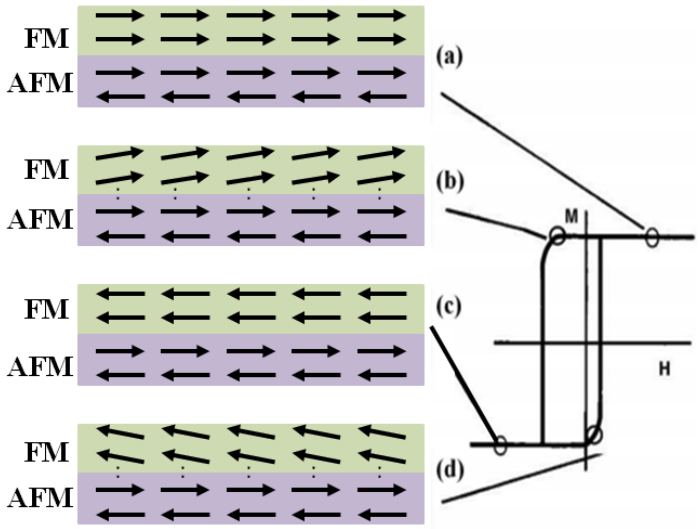

Figure 10. Spin configurations in an AFM-FM system at various platforms during the hysteresis loop for an AFM system with large magnetic anisotropy.

5. Magnetic Behaviour of Double Perovskites

5.1 Bulk Compounds of Double Perovskites

Earlier studies on R_2NiMnO_6 have been targeted to verify Goodenough-Kanamori's rules according to which ferromagnetism in a material may result by the interaction of one metal site vacant d-orbital along

with half-filled d orbital of another metal site via an anion through an exchange interaction which is 180° superexchange interaction. The assumption of these rules is that owing to greater cation anion overlap the contact of e_g orbitals will lead over interaction among t_{2g} orbitals. It was also found that LNMO is a FM semiconductor with ordered Ni^{2+} (d^8:$t_{2g}^6 e_g^2$) and Mn^{4+} (d^3: $t_{2g}^3\ e_g^0$) ions occupying the metal (M) centers of corner sharing MO_6 octahedra in a perovskite with structural distortion (Dass et al., 2003). Dass et al. (2003), prepared the La_2NiMnO_6 (LNMO) polycrystalline samples using different synthesis methods and studied their magnetic and transport properties. At high temperatures, LNMO possesses rhombohedral structure and at low temperatures it turns into a monoclinic structure (Rogado et al., 2005). The coexistence of these two structures has been observed over a large range of temperature including ambient temperature. The co-existence of structures is due to local inhomogeneities. Rogado et al. (2005), observed magnetoresistance and magnetocapacitance effect near room temperature in polycrystalline LNMO sample. Choudhary et al. (2012), prepared a partially disordered La_2NiMnO_6 by the Pechini method, which shows a reentrant spin-glass-like behaviour. There is a lot of studies on bulk La_2NiMnO_6 (Barbosa et al., 2016; Chandrasekhar et al., 2012; Choudhury et al., 2012; Guo et al., 2013; Kumar and Kaur, 2013). Nevertheless, other compounds of this group are less explored. Booth and colleagues (Booth et al., 2009), conducted a synthesis of a range of bulk RNMO compounds and thoroughly examined their structural, dielectric, and magnetic characteristics. Their findings indicated that a decrease in the ionic radius of rare earth element leads to changes in the Ni-O-Mn bond length and bond angle, both of which play direct roles in the exchange interactions. For instance, Yadav and Elizabeth (2015), observed the crystallization of NNMO occurs in monoclinic $P2_1/n$ symmetry which depending on synthesis parameters may be partially disordered. Shi et al. (2011), detected two transitions in magnetization versus temperature curves of NNMO polycrystalline sample. The first transition (~194 K) may be associated with Curie temperature of ferromagnetic character of NNMO caused by the superexchange interactions Ni^{2+} and Mn^{4+} ions i.e. Ni^{2+}-O-Mn^{4+}. The other transition observed (~105 K) may be associated to Ni^{3+}-O-Mn^{3+} superexchange interactions. The formation of ordered or disordered double perovskite structure is purely based on the synthesis conditions of the sample.

Apart from this, a substantial work has been done on A-site doping in these compounds. For instance, Guo et al. (2013), observed a tunable exchange bias effect in $La_{2-x}Sr_xNiMnO_6$ compound which increases with Sr doping. Kang et al. (2009), investigated the magnetic characteristics of $La_{2-x}Sr_xNiMnO_6$ and observed that the extent of ASDs increases with Sr-doping and hence the magnetization reduces. Murthy et al. (2016) studied the exchange bias effect in $La_{2-x}Sr_xCoMnO_6$ compound, which is induced by the antisite disorders. Consequence of Ca doping on the characteristics of polycrystalline La_2NiMnO_6 has been investigated by Guo et al. (2013b). As Ca-doping increases, there is a decrease in both the saturation magnetization and the transition temperature, both have been associated with the reduction of Ni–O–Mn bond angle and the enhancement in the amount of ASDs, respectively. ASDs-induced exchange bias phenomenon was studied by Singh et al. (2016) in polycrystalline samples of NNMO, however, they did not find any spin glass phase in the sample. Moreover, Singh and Chandra (2022) found a high value of T_C ~ 264 K in NdSrNiMnO6 nanoparticles, which is much greater than T_C (~194 K) of parent compound $Nd_2NiMnO6$. Additionally, they also observed particle size dependent EB phenomenon in NdSrNiMnO6 nanoparticles.

5.2 Thin Films of Double Perovskites

Thin films of double perovskite compounds are much superior over bulk compounds. The thin films of these compounds are promising candidates to be used in integrated devices, such as recording memories, spintronics, micro-electro-mechanical systems, and sensors. (Asano et al., 2004; Guo et al., 2008; Kumar and Kaur, 2011; Kumar and Kaur, 2013; Singh et al., 2007, 2009). To achieve these superior properties, it is highly desirable to prepare high quality thin films. This can be achieved by employing a wide different deposition methods like spin coating, sputtering, molecular beam epitaxy (MBE), pulsed laser deposition

(PLD), MOCVD and many more (Ma et al., 2011; Singh and Kumar, 2024). However, the traditional chemical methods are not applicable when there is a demand of high structural perfection for the synthesis of oxide thin films and customization of the oxide layer down to atomic level are required. Alternatively, to achieve good epitaxial growth and coherent interfaces, techniques like PLD, MBE and sputtering (physical vapor deposition) are preferred in which the thickness may be tuned at the atomic scale.

In PVD techniques e.g. PLD, the choice of substrate plays a substantial role to control the strain state and orientation of the epitaxial films (Kovachev and Wesselinowa, 2009; Ma et al., 2011). The Orientation of the thin films plays vital role in the morphology and crystallization of the multicomponent nanostructured thin films**.** Magnetic and structural properties of epitaxial LNMO thin films have been studied by Guo et al. (2008). In case of large lattice mismatch, the magnetic properties have been found to be strongly substrate dependent. STO, LSAT, and LAO substrates have been used to deposit double-perovskite structured epitaxial thin films of ferromagnetic LNMO (Guo et al., 2006). The magnetic and structural measurements reveal that for Ni^{2+} and Mn^{4+} ions there occurs a rock-salt-type ordering. Epitaxial LNMO films were deposited on STO and LSAT substrates in many situations by Sakurai et al. (2011), suggesting that the primary growth stage prominently affects the ferromagnetism of ordered perovskite films. Therefore, the selection of a single crystal substrate plays a vital role in achieving a much higher number of B-site ions ordering, which is essential for the epitaxial growth of ordered perovskite. PLD technique was utilized to grow LNMO thin films on $LaAlO_3$, $NdGaO_3$, $SrTiO_3$, and MgO substrates under different conditions of oxygen back- ground pressure (25–800 mTorr) (Guo et al., 2008). It has been observed that environment of oxygen while film deposition has a large influence on magnetic properties, chemical composition, and crystal structure of the films. The outcome of this study stresses the role of mixed cation valence and oxygen defects in finalizing the behaviour of the ferromagnetic LNMO compound and the requirement to wisely adjust the processing parameters so as to obtain the intrinsic properties (Guo et al., 2008). The structural and magnetic properties of LNMO thin films with varying film thickness has been systematically studied (Kumar and Kaur, 2013). A drastic change is observed in saturation magnetization and Curie temperature with increasing film thickness. Magnetic properties and the phonon behaviour of $Pr_2NiMnO6$ (PNMO) films were investigated by Singh et al. (2011). Furthermore, Epitaxial NNMO thin films were synthesized on STO substrate using the PLD technique with varying thickness by Singh et al. (2017b). In another study, they also investigated the effect of different substrates on the structural and magnetic properties of epitaxial NNMO thin films (Singh et al. 2017c). Singh et al. (2017a) also observed spin glass and exchange bias phenomena in epitaxial NNMO thin film, which is caused by the increasing amount of ASDs within the film owing to strain.

6. Conclusion

In summary, our investigation highlights the diverse magnetic properties offered by double perovskite compounds, characterized by the variation of both B and B' cations, in contrast to the single B cation present in perovskite compounds. The manipulation of chemical composition involving B and B' cations exert a significant influence on magnetic properties. Antisite disorders, inherent growth defects in double perovskite compounds, play a pivotal role in shaping their magnetic behaviour. It's noteworthy that first-principles calculations demonstrate a remarkable capability to elucidate the impact of chemical variations, providing a microscopic understanding of observed magnetic phenomena. This understanding serves as a valuable tool for both optimizing existing double perovskite materials and predicting novel compounds with enhanced magnetic properties. The identification of spin glass and Exchange bias phenomena across various types of double perovskite materials opens avenues for their application in spintronic device development. These phenomena are ascribed to the existence of antisite disorders within the double perovskite structure. Additionally, the finding of high Curie temperatures (T_C), approaching room temperature, in double perovskite compounds holds promise for practical applications in spintronics.

Conflict of Interest
No competing interests or personal relationships influencing the reported work are declared by the authors.

Acknowledgments
No acknowledgment was reported by the authors.

References

Aharen, T., Greedan, J.E., Bridges, C.A., Aczel, A.A., Rodriguez, J., MacDougall, G., Luke, G.M., Michaelis, V.K., Zhou, H., Wiebe, C.R., Cranswick, L.M.D. (2010). Magnetic properties of the geometrically frustrated S= 1 2 antiferromagnets, La 2 LiMoO 6 and Ba 2 YMoO 6, with the B-site ordered double perovskite structure: Evidence for a collective spin-singlet ground state. *Physical Review B—Condensed Matter and Materials Physics*, *81*(22), 224409. https://doi.org/10.1103/PhysRevB.81.224409.

Anderson, M.T., & Poeppelmeier, K.R. (1991). Lanthanum copper tin oxide (La2CuSnO6): A new perovskite-related compound with an unusual arrangement of B cations. *Chemistry of Materials*, *3*(3), 476-482.

Anderson, M.T., Greenwood, K.B., Taylor, G.A., & Poeppelmeier, K.R. (1993a). B-cation arrangements in double perovskites. *Progress in Solid State Chemistry*, *22*(3), 197-233.

Anderson, M.T., Poeppelmeier, K.R., Gramsch, S.A., & Burdett, J.K. (1993b). Structure-property relationships in the layered cuprate La2-xSrxCuSnO6. *Journal of Solid State Chemistry*, *102*(1), 164-174. https://doi.org/10.1006/jssc.1993.1019.

Asai, K., Fujiyoshi, K., Nishimori, N., Satoh, Y., Kobayashi, Y., & Mizoguchi, M. (1998). Magnetic Properties of REMe 0.5 Mn 0.5 O 3 (RE= Rare Earth Element, Me= Ni, Co). *Journal of the Physical Society of Japan*, *67*(12), 4218-4228. https://doi.org/10.1143/JPSJ.67.4218.

Asai, K., Kobayashi, N., Bairo, T., Kaneko, N., Kobayashi, Y., Suzuki, M., Satoh, Y., & Mizoguchi, M. (2005). 55Mn NMR in ferromagnetic perovskites RENi0. 5Mn0. 5O3 (RE= Rare earth element). *Journal of the Physical Society of Japan*, *74*(4), 1289-1296. https://doi.org/10.1143/JPSJ.74.1289.

Asano, H., Kozuka, N., Tsuzuki, A., & Matsui, M. (2004). Growth and properties of high-Curie-temperature Sr2CrReO6 thin films. *Applied Physics Letters*, *85*(2), 263-265. https://doi.org/10.1063/1.1769085.

Azad, A.K., Eriksson, S.G., Mellergård, A., Ivanov, S.A., Eriksen, J., & Rundlöf, H. (2002). A study on the nuclear and magnetic structure of the double perovskites A2FeWO6 (A= Sr, Ba) by neutron powder diffraction and reverse Monte Carlo modeling. *Materials Research Bulletin*, *37*(11), 1797-1813. https://doi.org/10.1016/S0025-5408(02)00872-3.

Azuma, M., Kaimori, S., & Takano, M. (1998). High-pressure synthesis and magnetic properties of layered double perovskites Ln2CuMO6 (Ln= La, Pr, Nd, and Sm; M= Sn and Zr). *Chemistry of Materials*, *10*(10), 3124-3130. https://doi.org/10.1021/cm980217g.

Azuma, M., Takata, K., Saito, T., Ishiwata, S., Shimakawa, Y., & Takano, M. (2005). Designed ferromagnetic, ferroelectric Bi2NiMnO6. *Journal of the American Chemical Society*, *127*(24), 8889-8892.

Balasubramanian, P., Joshi, S.R., Yadav, R., de Groot, F.M., Singh, A.K., Ray, A., Maitra, T., & Malik, V. (2018). Electronic structure of Pr2MnNiO6 from x-ray photoemission, absorption and density functional theory. *Journal of Physics: Condensed Matter*, *30*(43), 435603.

Barbosa, D.A., Lufaso, M.W., Reichlova, H., Marti, X., Rezende, M.V., Maciel, A.P., & Paschoal, C.W. (2016). Ba-doping effects on structural, magnetic and vibrational properties of disordered La2NiMnO6. *Journal of Alloys and Compounds*, *663*, 899-905. https://doi.org/10.1016/j.jallcom.2015.11.099.

Bardelli, F., Meneghini, C., Mobilio, S., Ray, S., & Sarma, D.D. (2009). Local structure of Sr2FeMoxW1−xO6 double perovskites across the composition-driven metal to insulator transition. *Journal of Physics: Condensed Matter*, *21*(19), 195502. https://doi.org/10.1088/0953-8984/21/19/195502.

Bedanta, S., & Kleemann, W. (2008). Supermagnetism. *Journal of Physics D: Applied Physics*, *42*(1), 013001. https://doi.org/10.1088/0022-3727/42/1/013001.

Bednorz, J.G., & Müller, K.A. (1986). Possible high T c superconductivity in the Ba− La− Cu− O system. *Zeitschrift für Physik B Condensed Matter*, *64*(2), 189-193. https://doi.org/10.1007/BF01303701.

Berkowitz, A.E., & Takano, K. (1999). Exchange anisotropy—a review. *Journal of Magnetism and Magnetic Materials*, *200*(1-3), 552-570. https://doi.org/10.1016/S0304-8853(99)00453-9.

Binder, K., & Young, A.P. (1986). Spin glasses: Experimental facts, theoretical concepts, and open questions. *Reviews of Modern Physics*, *58*(4), 801-976. https://doi.org/10.1103/RevModPhys.58.801.

Blackstead, H.A., Dow, J.D., Harshman, D.R., Yelon, W.B., Chen, M.X., Wu, M.K., Wu, D.Y., Chen, F. Z., Chien, & Pulling, D.B. (2001). Magnetically ordered Cu and Ru in Ba 2 GdRu 1− u Cu u O 6 and in Sr 2 YRu 1− u Cu u O 6. *Physical Review B*, *63*(21), 214412. https://doi.org/10.1103/PhysRevB.63.214412.

Booth, R.J., Fillman, R., Whitaker, H., Nag, A., Tiwari, R.M., Ramanujachary, K.V., Gopalakrishnan, J., & Lofland, S.E. (2009). An investigation of structural, magnetic and dielectric properties of R2NiMnO6 (R= rare earth, Y). *Materials Research Bulletin*, *44*(7), 1559-1564. https://doi.org/10.1016/j.materresbull.2009.02.003.

Bray, A.J., & Moore, M.A. (1987). Chaotic nature of the spin-glass phase. *Physical Review Letters*, *58*(1), 57-60. https://doi.org/10.1103/PhysRevLett.58.57.

Brixner, L.H. (1960). Preparation and structure determination OF some new CUBIC and tetragonally -distorted perovskites. *The Journal of Physical Chemistry*, *64*(1), 165-166.

Bull, C.L., & McMillan, P.F. (2004). Raman scattering study and electrical properties characterization of elpasolite perovskites Ln2 (BB′) O6 (Ln= La, Sm… Gd and B, B′= Ni, Co, Mn). *Journal of Solid State Chemistry*, *177*(7), 2323-2328. https://doi.org/10.1016/j.jssc.2004.02.022.

Čebela, M., Zagorac, D., Batalović, K., Radaković, J., Stojadinović, B., Spasojević, V., & Hercigonja, R. (2017). BiFeO3 perovskites: A multidisciplinary approach to multiferroics. *Ceramics International*, *43*(1), 1256-1264. https://doi.org/10.1016/j.ceramint.2016.10.074.

Chandrasekhar, K.D., Das, A.K., Mitra, C., & Venimadhav, A. (2012). The extrinsic origin of the magnetodielectric effect in the double perovskite La2NiMnO6. *Journal of Physics: Condensed Matter*, *24*(49), 495901. https://doi.org/10.1088/0953-8984/24/49/495901.

Chaturvedi, S., Shirolkar, M.M., Rajendra, R., Singh, S., Ballav, N., & Kulkarni, S. (2014). Coercivity and exchange bias of bismuth ferrite nanoparticles isolated by polymer coating. *Journal of Applied Physics*, *115*, 123906. https://doi.org/10.1063/1.4869657.

Chauhan, S., Singh, A.K., Srivastava, S.K., & Chandra, R. (2016). Study of magnetic behavior in hexagonal-YMn1−xFexO3 (x= 0 and 0.2) nanoparticles using remanent magnetization curves. *Journal of Magnetism and Magnetic Materials*, *414*, 187-193. https://doi.org/10.1016/j.jmmm.2016.04.074.

Choudhury, D., Mandal, P., Mathieu, R., Hazarika, A., Rajan, S., Sundaresan, A., & Sarma, D.D. (2012). Near-room-temperature colossal magnetodielectricity and multiglass properties<? format?> in partially disordered La 2 NiMnO 6. *Physical Review Letters*, *108*(12), 127201. https://doi.org/10.1103/PhysRevLett.108.127201.

Dass, R.I., Yan, J.Q., & Goodenough, J.B. (2003). Oxygen stoichiometry, ferromagnetism, and transport properties of La 2− x NiMnO 6+ δ. *Physical Review B*, *68*(6), 064415. https://doi.org/10.1103/PhysRevB.68.064415.

de Vries, M.A., Mclaughlin, A.C., & Bos, J.W. (2010). Valence bond glass on an fcc lattice in the double perovskite Ba 2 YMoO 6. *Physical Review Letters*, *104*(17), 177202. https://doi.org/10.1103/PhysRevLett.104.177202.

Fresia, E.J., Katz, L., & Ward, R. (1959). Cation Substitution in perovskite-like phases1, 2. *Journal of the American Chemical Society*, *81*(18), 4783-4785.

Gajek, M., Bibes, M., Barthélémy, A., Bouzehouane, K., Fusil, S., Varela, M., Fontcuberta, J., & Fert, A. (2005). Spin filtering through ferromagnetic Bi Mn O 3 tunnel barriers. *Physical Review B—Condensed Matter and Materials Physics*, *72*(2), 020406. https://doi.org/10.1103/PhysRevB.72.020406.

Galasso, F., Katz, L., & Ward, R. (1959). Substitution in the octahedrally coördinated cation positions in compounds of the perovskite type1, 2. *Journal of the American Chemical Society*, *81*(4), 820-823. https://doi.org/10.1021/ja01513a018.

Galstyan, E., Xue, Y., Iliev, M., Sun, Y., & Chu, C.W. (2007). Origin of the superconductivity in the Y-Sr-Ru-O and Y-Sr-Cu-O systems. *Physical Review B—Condensed Matter and Materials Physics*, *76*(1), 014501. https://doi.org/10.1103/PhysRevB.76.014501.

Garcıa-Landa, B., Ritter, C., Ibarra, M.R., Blasco, J., Algarabel, P.A., Mahendiran, R., & Garcıa, J. (1999). Magnetic and magnetotransport properties of the ordered perovskite Sr2FeMoO6. *Solid State Communications*, *110*(8), 435-438. https://doi.org/10.1016/S0038-1098(99)00079-4.

Glazer, A.M. (1972). The classification of tilted octahedra in perovskites. *Acta Crystallographica Section B: Structural Crystallography and Crystal Chemistry*, *28*(11), 3384-3392. https://doi.org/10.1107/S0567740872007976.

Goldschmidt, V.M. (1926). Die gesetze der krystallochemie. *Naturwissenschaften*, *14*(21), 477-485. https://doi.org/10.1007/BF01507527.

Goodenough, J.B. (1955). Theory of the role of covalence in the perovskite-type manganites [La, M (II)] Mn O 3. *Physical Review*, *100*(2), 564-573. https://doi.org/10.1103/PhysRev.100.564.

Graf, T., Felser, C., & Parkin, S.S. (2011). Simple rules for the understanding of Heusler compounds. *Progress in Solid State Chemistry*, *39*(1), 1-50. https://doi.org/10.1016/j.progsolidstchem.2011.02.001.

Guo, H., Burgess, J., Street, S., Gupta, A., Calvarese, T.G., & Subramanian, M.A. (2006). Growth of epitaxial thin films of the ordered double perovskite La2NiMnO6 on different substrates. *Applied Physics Letters*, *89*(2), 22509. https://doi.org/10.1063/1.2221894.

Guo, H.Z., Burgess, J., Ada, E., Street, S., Gupta, A., Iliev, M.N., Kellock, C., Varela, M., & Pennycook, S.J. (2008). Influence of defects on structural and magnetic properties of multifunctional La 2 Ni Mn O 6 thin films. *Physical Review B—Condensed Matter and Materials Physics*, *77*(17), 174423. https://doi.org/10.1103/PhysRevB.77.174423.

Guo, Y., Shi, L., Zhou, S., Zhao, J., & Liu, W. (2013a). Near room-temperature magnetoresistance effect in double perovskite La2NiMnO6. *Applied Physics Letters*, *102*, 222401. https://doi.org/10.1063/1.4808437.

Guo, Y., Shi, L., Zhou, S., Zhao, J., & Wei, S. (2013b). Local valence and hole-doping effect on magnetic properties in double perovskite La 2 NiMnO 6. *Journal of Superconductivity and Novel Magnetism*, *26*, 3287-3292. https://doi.org/10.1007/s10948-013-2168-6.

Guo, Y., Shi, L., Zhou, S., Zhao, J., Wang, C., Liu, W., & Wei, S. (2013c). Tunable exchange bias effect in Sr-doped double perovskite La2NiMnO6. *Journal of Physics D: Applied Physics*, *46*(17), 175302. https://doi.org/10.1088/0022-3727/46/17/175302.

Guo, Y., Xiao, P., Luo, L., Jiang, N., Lei, F., Zheng, Q., & Lin, D. (2014). Structure, ferroelectric and piezoelectric properties of Bi 0.5 (Na 0.8 K 0.2) 0.5 TiO 3 modified BiFeO 3–BaTiO 3 lead-free piezoelectric ceramics. *Journal of Materials Science: Materials in Electronics*, *25*, 3753-3761. https://doi.org/10.1007/s10854-014-2086-9.

Haskel, D., Fabbris, G., Souza-Neto, N.M., Van Veenendaal, M., Shen, G., Smith, A.E., & Subramanian, M.A. (2011). Stability of the ferromagnetic ground state of La 2 MnNiO 6 against large compressive stress. *Physical Review B—Condensed Matter and Materials Physics*, *84*(10), 100403. https://doi.org/10.1103/PhysRevB.84.100403.

Hrkac, V., Lage, E., Köppel, G., Strobel, J., McCord, J., Quandt, E., Meyners, D., & Kienle, L. (2014). Amorphous FeCoSiB for exchange bias coupled and decoupled magnetoelectric multilayer systems: Real-structure and magnetic properties. *Journal of Applied Physics*, *116*(13). https://doi.org/10.1063/1.4896662.

Husain, S., Kumar, A., Akansel, S., Svedlindh, P., & Chaudhary, S. (2017). Anomalous hall effect in ion-beam sputtered Co2FeAl full Heusler alloy thin films. *Journal of Magnetism and Magnetic Materials*, *442*, 288-294. https://doi.org/10.1016/j.jmmm.2017.06.127.

Imada, M., Fujimori, A., & Tokura, Y. (1998). Metal-insulator transitions. *Reviews of Modern Physics*, *70*(4), 1039-1263. https://doi.org/10.1103/RevModPhys.70.1039.

Itoh, M., Ohta, I., & Inaguma, Y. (1996). Valency pair and properties of 1: 1 ordered perovskite-type compounds Sr2MMoO6 (M= Mn, Fe, Co). *Materials Science and Engineering: B*, *41*(1), 55-58. https://doi.org/10.1016/S0921-5107(96)01623-6.

Joly, V.J., Joy, P.A., Date, S.K., & Gopinath, C.S. (2002). Two ferromagnetic phases with different spin states of Mn and Ni in LaMn 0.5 Ni 0.5 O 3. *Physical Review B*, *65*(18), 184416. https://doi.org/10.1103/PhysRevB.65.184416.

Jonker, G.H., & Van Santen, J.H. (1950). Ferromagnetic compounds of manganese with perovskite structure. *Physica*, *16*(3), 337-349. https://doi.org/10.1016/0031-8914(50)90033-4.

Kanamori, J. (1959). Superexchange interaction and symmetry properties of electron orbitals. *Journal of Physics and Chemistry of Solids*, *10*(2-3), 87-98.

Kang, J.S., Lee, H.J., Kim, D.H., Kolesnik, S., Dabrowski, B., Świerczek, K., & Min, B.I. (2009). Valence and spin states, and the metal-insulator transition in ferromagnetic La 2− x Sr x MnNiO 6 (x= 0, 0.2). *Physical Review B—Condensed Matter and Materials Physics*, *80*(4), 045115. https://doi.org/10.1103/PhysRevB.80.045115.

Kato, H., Okuda, T., Okimoto, Y., Tomioka, Y., Takenoya, Y., Ohkubo, A., Kawasaki, M., & Tokura, Y. (2002). Metallic ordered double-perovskite Sr2CrReO6 with maximal Curie temperature of 635 K. *Applied Physics Letters*, *81*(2), 328-330. https://doi.org/10.1063/1.1493646.

Kawasaki, J.K., Chatterjee, S., Canfield, P.C., & Guest Editors. (2022). Full and half-Heusler compounds. *MRS Bulletin*, *47*(6), 555-558. https://doi.org/10.1557/s43577-022-00355-w.

Kim, S.B., Lee, B.W., & Kim, C.S. (2002). Neutron and Mössbauer studies of the double perovskite A2FeMoO6 (A= Sr and Ba). *Journal of Magnetism and Magnetic Materials*, *242*, 747-750. https://doi.org/10.1016/S0304-8853(01)01015-0.

Kim, Y., Lee, S.J., Han, W.B., Kim, H.S., An, H.H., & Yoon, C.S. (2013). Structure and magnetic properties of low-temperature annealed Ni-Mn-Al alloys. *Journal of Applied Physics*, *113*(17), 17B102. https://doi.org/10.1063/1.4795323.

Kimura, T., Goto, T., Shintani, H., Ishizaka, K., Arima, T.H., & Tokura, Y. (2003a). Magnetic control of ferroelectric polarization. *Nature*, *426*(6962), 55-58. https://doi.org/10.1038/nature02018.

Kimura, T., Kawamoto, S., Yamada, I., Azuma, M., Takano, M., & Tokura, Y. (2003b). Magnetocapacitance effect in multiferroic BiMnO 3. *Physical Review B*, *67*(18), 180401. https://doi.org/10.1103/PhysRevB.67.180401.

Kiwi, M. (2001). Exchange bias theory. *Journal of Magnetism and Magnetic Materials*, *234*(3), 584-595. https://doi.org/10.1016/S0304-8853(01)00421-8.

Kobayashi, K.I., Kimura, T., Sawada, H., Terakura, K., & Tokura, Y. (1998). Room-temperature magnetoresistance in an oxide material with an ordered double-perovskite structure. *Nature*, *395*(6703), 677-680. https://doi.org/10.1038/27167.

Kovachev, S., & Wesselinowa, J.M. (2009). Influence of substrate effects on the properties of multiferroic thin films. *Journal of Physics: Condensed Matter*, *21*(39), 395901. https://doi.org/10.1088/0953-8984/21/39/395901.

Kumar, A., Sanger, A., Singh, A.K., Kumar, A., Kumar, M., & Chandra, R. (2017). Experimental evidence of spin glass and exchange bias behavior in sputtered grown α-MnO2 nanorods. *Journal of Magnetism and Magnetic Materials*, *433*, 227-233. https://doi.org/10.1016/j.jmmm.2017.02.061.

Kumar, D., & Kaur, D. (2011). Exchange biasing in SFMO/SFWO double perovskite multilayer thin films. *Journal of Alloys and Compounds*, *509*(30), 7886-7890. https://doi.org/10.1016/j.jallcom.2011.05.006.

Kumar, D., & Kaur, D. (2013). Structural and magnetic properties of La2NiMnO6 thin films on LaAlO3 substrate with varying thickness. *Journal of Alloys and Compounds*, *554*, 277-283. https://doi.org/10.1016/j.jallcom.2012.10.065.

Li, H., Sun, L.P., Li, Q., Xia, T., Zhao, H., Huo, L.H., Bassat, J.M., Rougier, A., Fourcade, S., & Grenier, J.C. (2015). Electrochemical performance of double perovskite Pr2NiMnO6 as a potential IT-SOFC cathode. *International Journal of Hydrogen Energy*, *40*(37), 12761-12769. https://doi.org/10.1016/j.ijhydene.2015.07.133.

Lu, Y.W., & Qi, X. (2019). Hydrothermal synthesis of pure and Sb-doped BiFeO3 with the typical hysteresis loops of ideal ferroelectrics. *Journal of Alloys and Compounds*, *774*, 386-395. https://doi.org/10.1016/j.jallcom.2018.09.374.

Ma, J., Hu, J., Li, Z., & Nan, C.W. (2011). Recent progress in multiferroic magnetoelectric composites: from bulk to thin films. *Advanced Materials*, *23*(9), 1062-1087. https://doi.org/10.1002/adma.201003636.

McCord, J., & Mangin, S. (2013). Separation of low-and high-temperature contributions to the exchange bias in Ni 81 Fe 19-NiO thin films. *Physical Review B—Condensed Matter and Materials Physics*, *88*(1), 014416. https://doi.org/10.1103/PhysRevB.88.014416.

Meiklejohn, W.H., & Bean, C.P. (1956). New magnetic anisotropy. *Physical Review*, *102*(5), 1413.

Mishra, A., Srivastava, S.K., Kumar, A., Dubey, P., Chauhan, S., Singh, A.K., Kaur, D., & Chandra, R. (2014). Thickness dependent exchange bias in co-sputter deposited Ni–Mn–Al Heusler alloy hard nanostructured thin films. *Thin Solid Films*, *572*, 142-146. https://doi.org/10.1016/j.tsf.2014.08.014.

Mouallem-Bahout, M., Roisnel, T., André, G., Gutierrez, D., Moure, C., & Peña, O. (2004). Nuclear and magnetic order in Y (Ni, Mn) O3 manganites by neutron powder diffraction. *Solid State Communications*, *129*(4), 255-260. https://doi.org/10.1016/j.ssc.2003.09.039.

Moya, X., Mañosa, L., Planes, A., Krenke, T., Acet, M., Garlea, V.O., Lograsso, T.A., Schlagel, D.L., & Zarestky, J. L. (2006). Lattice dynamics and phonon softening in Ni-Mn-Al Heusler alloys. *Physical Review B—Condensed Matter and Materials Physics*, *73*(6), 064303. https://doi.org/10.1103/PhysRevB.73.064303.

Murthy, J.K., & Venimadhav, A. (2013). Giant zero field cooled spontaneous exchange bias effect in phase separated La1. 5Sr0. 5CoMnO6. *Applied Physics Letters*, *103*, 252410. ttps://doi.org/10.1063/1.4855135.

Murthy, J.K., Chandrasekhar, K.D., Wu, H.C., Yang, H.D., Lin, J.Y., & Venimadhav, A. (2016). Antisite disorder driven spontaneous exchange bias effect in La2− xSrxCoMnO6 (0⩽ x⩽ 1). *Journal of Physics: Condensed Matter*, *28*(8), 086003. https://doi.org/10.1088/0953-8984/28/8/086003.

Nair, H.S., Pradheesh, R., Xiao, Y., Cherian, D., Elizabeth, S., Hansen, T., Chatterji, T., & Brückel, T. (2014). Magnetization-steps in Y2CoMnO6 double perovskite: the role of antisite disorder. *Journal of Applied Physics*, *116*(12), 123907. https://doi.org/10.1063/1.4896399.

Nair, S.G., Satapathy, J., & Kumar, N.P. (2020). Influence of synthesis, dopants, and structure on electrical properties of bismuth ferrite (BiFeO 3). *Applied Physics A*, *126*(11), 836. https://doi.org/10.1007/s00339-020-04027-x.

Nogués, J., & Schuller, I.K. (1999). Exchange bias. *Journal of Magnetism and Magnetic Materials*, *192*(2), 203-232. https://doi.org/10.1016/S0304-8853(98)00266-2.

Pradheesh, R., Nair, H.S., Kumar, C.M.N., Lamsal, J., Nirmala, R., Santhosh, P.N., Yelon, W.B., Malik, S.K., Sankaranarayanan, V., & Sethupathi, K. (2012). Observation of spin glass state in weakly ferromagnetic Sr2FeCoO6 double perovskite. *Journal of Applied Physics*, *111*, 53905. https://doi.org/10.1063/1.3686137.

Rogado, N.S., Li, J., Sleight, A.W., & Subramanian, M.A. (2005). Magnetocapacitance and magnetoresistance near room temperature in a ferromagnetic semiconductor: La2NiMnO6. *Advanced Materials*, *17*(18), 2225-2227. https://doi.org/10.1002/adma.200500737.

Saha-Dasgupta, T. (2013). Magnetism in double perovskites. *Journal of Superconductivity and Novel Magnetism*, *26*, 1991-1995. https://doi.org/10.1007/s10948-012-2070-7.

Sahoo, R.C., Giri, S.K., Dasgupta, P., Poddar, A., & Nath, T.K. (2016). Exchange bias effect in ferromagnetic LaSrCoMnO6 double perovskite: Consequence of spin glass-like ordering at low temperature. *Journal of Alloys and Compounds*, *658*, 1003-1009. https://doi.org/10.1016/j.jallcom.2015.11.025.

Sakurai, Y., Ohkubo, I., Matsumoto, Y., Koinuma, H., & Oshima, M. (2011). Influence of substrates on epitaxial growth of B-site-ordered perovskite La2NiMnO6 thin films. *Journal of Applied Physics*, *110*, 63913. https://doi.org/10.1063/1.3641982.

Salamon, M.B., & Jaime, M. (2009). The physics of manganites: Structure and transport. *Reviews of Modern Physics*, *73*(3), 583-628.

Sanyal, P., Tarat, S., & Majumdar, P. (2008). Structural ordering and antisite defect formation in double perovskites. *The European Physical Journal B*, *65*, 39-47. https://doi.org/10.1140/epjb/e2008-00327-2.

Sarma, D.D., Shanthi, N., & Mahadevan, P. (1996). Electronic excitation spectra from ab initio band-structure results for LaM O 3 (M= Cr, Mn, Fe, Co, Ni). *Physical Review B*, *54*(3), 1622. http://link.aps.org/doi/10.1103/PhysRevB.54.1622.

Schmitz-DuMont, O., & Kasper, H. (1965). Über eine neue Klasse quarternärer Oxide von Typus M II M III lnO 4. Die Lichtabsorption des 2-wertigen Kupfers, Nickels und Kobalts sowie des 3-wertigen Chroms. *Zeitschrift für Anorganische und Allgemeine Chemie*, *341*(5-6), 252-268.

Serrate, D., De Teresa, J.M., & Ibarra, M.R. (2006). Double perovskites with ferromagnetism above room temperature. *Journal of Physics: Condensed Matter*, *19*(2), 023201. https://doi.org/10.1088/0953-8984/19/2/023201.

Sharif, S., Murtaza, G., Khan, M.A., Sadaf, A., Al-Muhimeed, T.I., & Nazir, G. (2021). Tailoring the multiferroic properties of BiFeO3 by low energy ions implantation. *Journal of Electroceramics*, *47*(3), 100-117. https://doi.org/10.1007/s10832-021-00258-3.

Sharma A.H., Barman, R., Kaur, N., Choudhary, N., & Kaur, D. (2013a). Exchange bias effect in NiMnSb/CrN heterostructures deposited by magnetron sputtering. *Journal of Applied Physics*, *113*(17), 1-4. https://doi.org/10.1063/1.4798373.

Sharma, G., Saha, J., Kaushik, S.D., Siruguri, V., & Patnaik, S. (2013b). Magnetism driven ferroelectricity above liquid nitrogen temperature in Y2CoMnO6. *Applied Physics Letters*, *103*, 012903. https://doi.org/10.1063/1.4812728.

Shi, C., Hao, Y., & Hu, Z. (2011). Local valence and physical properties of double perovskite Nd2NiMnO6. *Journal of Physics D: Applied Physics*, *44*(24), 245405. https://doi.org/10.1088/0022-3727/44/24/245405.

Singh, A.K., & Chandra, R. (2018). Thickness dependent interfacial magnetic coupling in [La2NiMnO6/LaMnO3] multilayers. *Journal of Magnetism and Magnetic Materials*, *448*, 180-185. https://doi.org/10.1016/j.jmmm.2017.08.080.

Singh, A.K., & Chandra, R. (2022). Spin glass and exchange bias phenomena in NdSrNiMnO6 nanoparticles: Role of antiferromagnetic antisite disorders. *Journal of Magnetism and Magnetic Materials*, *549*, 169048. https://doi.org/10.1016/j.jmmm.2022.169048.

Singh, A.K., Balasubramanian, P., Singh, A., Gupta, M.K., & Chandra, R. (2018). Structural transformation, Griffiths phase and metal-insulator transition in polycrystalline Nd2− xSrxNiMnO6 (x= 0, 0.2, 0.4, 0.5 and 1) compound. *Journal of Physics: Condensed Matter*, *30*(35), 355401.

Singh, A.K., Chauhan, S., & Chandra, R. (2017a). Antisite disorder induced spin glass and exchange bias effect in Nd2NiMnO6 epitaxial thin film. *Applied Physics Letters*, *110*, 102402. https://doi.org/10.1063/1.4978354.

Singh, A.K., Chauhan, S., & Chandra, R. (2017b). Thickness dependent structural and magnetic properties of Nd2NiMnO6 epitaxial thin films. *Thin Solid Films*, *625*, 17-23. https://doi.org/10.1016/j.tsf.2017.01.056.

Singh, A.K., Chauhan, S., Balasubramanian, P., Srivastava, S.K., & Chandra, R. (2017c). Influence of substrate induced strain on B-site ordering and magnetic properties of Nd2NiMnO6 epitaxial thin films. *Thin Solid Films*, *629*, 49-54. https://doi.org/10.1016/j.tsf.2017.03.048.

Singh, A.K., Chauhan, S., Srivastava, S.K., & Chandra, R. (2016). Influence of antisite disorders on the magnetic properties of double perovskite Nd2NiMnO6. *Solid State Communications*, *242*, 74-78. https://doi.org/10.1016/j.ssc.2016.04.020.

Singh, A.K., Kumar, A. (2024). Experimental techniques for the characterization of magnetic thin films. *Prabha Materials Science Letters*, *3*(1),146-174. https://doi.org/10.33889/pmsl.2024.3.1.010.

Singh, B.P., Chaudhary, M., Kumar, A., Singh, A.K., Gautam, Y.K., Rani, S., & Walia, R. (2020). Effect of Co and Mn doping on the morphological, optical and magnetic properties of CuO nanostructures. *Solid State Sciences*, *106*, 106296.

Singh, D.J., & Park, C.H. (2008). Polar behavior in a magnetic perovskite from A-site size disorder: A density functional study. *Physical Review Letters*, *100*(8), 087601. https://doi.org/10.1103/PhysRevLett.100.087601.

Singh, M.P., Grygiel, C., Sheets, W.C., Boullay, P., Hervieu, M., Prellier, W., & Raveau, B. (2007). Absence of long-range Ni⁄ Mn ordering in ferromagnetic La2NiMnO6 thin films. *Applied Physics Letters*, *91*, 12503.

Singh, M.P., Truong, K.D., Jandl, S., & Fournier, P. (2009). Long-range Ni/Mn structural order in epitaxial double perovskite La 2 NiMnO 6 thin films. *Physical Review B—Condensed Matter and Materials Physics*, *79*(22), 224421. https://doi.org/10.1103/PhysRevB.79.224421.

Singh, M.P., Truong, K.D., Jandl, S., & Fournier, P. (2010). Multiferroic double perovskites: Opportunities, issues, and challenges. *Journal of Applied Physics*, *107*, 09D917. https://doi.org/10.1063/1.3362922.

Singh, M.P., Truong, K.D., Jandl, S., & Fournier, P. (2011). Magnetic properties and phonon behavior of Pr2NiMnO6 thin films. *Applied Physics Letters*, *98*, 162506. https://doi.org/10.1063/1.3575564.

Sung, K.D., Park, Y.A., Seo, M.S., Jo, Y., Hur, N., & Jung, J.H. (2012). Observation of intriguing exchange bias in BiFeO3 thin films. *Journal of Applied Physics*, *112*(3), 33915. https://doi.org/10.1063/1.4745887.

Tomioka, Y., Okuda, T., Okimoto, Y., Kumai, R., Kobayashi, K.I., & Tokura, Y. (2000). Magnetic and electronic properties of a single crystal of ordered double perovskite Sr 2 FeMoO 6. *Physical Review B*, *61*(1), 422-427. https://doi.org/10.1103/PhysRevB.61.422.

Torrance, J.B., Lacorre, P., Nazzal, A.I., Ansaldo, E.J., & Niedermayer, C. (1992). Systematic study of insulator-metal transitions in perovskites R NiO 3 (R= Pr, Nd, Sm, Eu) due to closing of charge-transfer gap. *Physical Review B*, *45*(14), 8209-8212. https://doi.org/10.1103/PhysRevB.45.8209.

Truong, K.D., Laverdière, J., Singh, M., Jandl, S., & Fournier, P. (2007). Impact of Co⁄Mn cation ordering on phonon anomalies in La 2 Co Mn O 6 double perovskites: Raman spectroscopy. *Physical Review B—Condensed Matter and Materials Physics*, *76*(13), 132413. https://doi.org/10.1103/PhysRevB.76.132413.

Vasala, S., & Karppinen, M. (2015). A2B′ B ″O6 perovskites: A review. *Progress in Solid State Chemistry*, *43*(1-2), 1-36. https://doi.org/10.1016/j.progsolidstchem.2014.08.001.

Vashisth, B.K., Bangruwa, J.S., Beniwal, A., Gairola, S.P., Kumar, A., Singh, N., & Verma, V. (2017). Modified ferroelectric/magnetic and leakage current density properties of Co and Sm co-doped bismuth ferrites. *Journal of Alloys and Compounds*, *698*, 699-705. https://doi.org/10.1016/j.jallcom.2016.12.278.

Vijayasundaram, S.V., Suresh, G., Mondal, R.A., & Kanagadurai, R. (2016). Substitution-driven enhanced magnetic and ferroelectric properties of BiFeO3 nanoparticles. *Journal of Alloys and Compounds*, *658*, 726-731.

von Helmolt, R., Wecker, J., Holzapfel, B., Schultz, L., & Samwer, K. (1993). Giant negative magnetoresistance in perovskitelike La 2/3 Ba 1/3 MnO x ferromagnetic films. *Physical Review Letters*, *71*(14), 2331.

Wang, X., Sui, Y., Li, Y., Li, L., Zhang, X., Wang, Y., Liu, Z., Su, W., & Tang, J. (2009). The influence of the antiferromagnetic boundary on the magnetic property of La2NiMnO6. *Applied Physics Letters*, *95*, 252502.

Yadav, A., & Chaudhary, S. (2015). Effect of growth temperature on the electronic transport and anomalous Hall effect response in co-sputtered Co2FeSi thin films. *Journal of Applied Physics*, *118*, 193902. https://doi.org/10.1063/1.4935823.

Yadav, R., & Elizabeth, S. (2015). Magnetic frustration and dielectric relaxation in insulating Nd2NiMnO6 double perovskites. *Journal of Applied Physics*, *117*, 53902. https://doi.org/10.1063/1.4906989.

Yang, W.Z., Liu, X.Q., Zhao, H.J., Lin, Y.Q., & Chen, X.M. (2012). Structure, magnetic, and dielectric characteristics of Ln2NiMnO6 (Ln= Nd and Sm) ceramics. *Journal of Applied Physics*, *112*, 64104. https://doi.org/10.1063/1.4752262.

Zener, C. (1951). Interaction between the d shells in the transition metals. *Physical Review*, *81*(3), 440-441. https://doi.org/10.1103/PhysRev.81.440.

Zhang, G.D., Dai, J.Q., & Liang, X.L. (2023). Enhanced ferroelectric properties in La -doped BiFeO3 films by the sol-gel method. *Journal of Sol-Gel Science and Technology*, *105*(2), 489-499. https://doi.org/10.1007/s10971-022-06009-2.

Zhong, W., Au, C.T., & Du, Y.W. (2013). Review of magnetocaloric effect in perovskite-type oxides. *Chinese Physics B*, *22*(5), 057501. https://doi.org/10.1088/1674-1056/22/5/057501.

Zhou, L., Zhang, Y., Li, S., Lian, Q., Yang, J., Bai, W., & Tang, X. (2020). Fe doping effect on the structural, ferroelectric and magnetic properties of polycrystalline BaTi 1− x Fe x O 3 ceramics. *Journal of Materials Science: Materials in Electronics*, *31*, 14487-14493. https://doi.org/10.1007/s10854-020-04008-z.

Zhou, S., Guo, Y., Zhao, J., He, L., & Shi, L. (2011). Size-induced Griffiths phase and second-order ferromagnetic transition in Sm0. 5Sr0. 5MnO3 nanoparticles. *The Journal of Physical Chemistry C*, *115*(5), 1535-1540. https://doi.org/10.1021/jp108553r.

Publisher's Note- Ram Arti Publishers remains neutral regarding jurisdictional claims in published maps and institutional affiliations.